Protein Science (1994), *3*:2280–2293. Cambridge University Press. Printed in the USA.

Structure–function analysis of human IL-6: Identification of two distinct regions that are important for receptor binding

ANNET HAMMACHER,[1] LARRY D. WARD,[1,5] JANET WEINSTOCK,[2] HERBERT TREUTLEIN,[3] KIYOSHI YASUKAWA,[4] AND RICHARD J. SIMPSON[1]

[1] Joint Protein Structure Laboratory, Ludwig Institute for Cancer Research/Walter and Eliza Hall Institute of Medical Research, Parkville, Victoria 3050, Australia
[2] Ludwig Institute for Cancer Research, Parkville, Victoria 3050, Australia
[3] Cooperative Research Centre for Cellular Growth Factors, Parkville, Victoria 3050, Australia
[4] Biotechnology Research Laboratory, Tosoh Corporation, Ayase-shi, Kanagawa 252, Japan

(RECEIVED April 18, 1994; ACCEPTED September 9, 1994)

Abstract

Interleukin-6 (IL-6) is a multifunctional cytokine that plays an important role in host defense. It has been predicted that IL-6 may fold as a 4 α-helix bundle structure with up-up-down-down topology. Despite a high degree of sequence similarity (42%) the human and mouse IL-6 polypeptides display distinct species-specific activities. Although human IL-6 (hIL-6) is active in both human and mouse cell assays, mouse IL-6 (mIL-6) is not active on human cells. Previously, we demonstrated that the 5 C-terminal residues of mIL-6 are important for activity, conformation, and stability (Ward LD et al., 1993, *Protein Sci 2*:1472–1481). To further probe the structure–function relationship of this cytokine, we have constructed several human/mouse IL-6 hybrid molecules. Restriction endonuclease sites were introduced and used to ligate the human and mouse sequences at junction points situated at Leu-62 (Lys-65 in mIL-6) in the putative connecting loop AB between helices A and B, at Arg-113 (Val-117 in mIL-6) at the N-terminal end of helix C, at Lys-150 (Asp-152 in mIL-6) in the connecting loop CD between helices C and D, and at Leu-178 (Thr-180 in mIL-6) in helix D. Hybrid molecules consisting of various combinations of these fragments were constructed, expressed, and purified to homogeneity.

The conformational integrity of the IL-6 hybrids was assessed by far-UV CD. Analysis of their biological activity in a human bioassay (using the HepG2 cell line), a mouse bioassay (using the 7TD1 cell line), and receptor binding properties indicates that at least 2 regions of hIL-6, residues 178–184 in helix D and residues 63–113 in the region incorporating part of the putative connecting loop AB through to the beginning of helix C, are critical for efficient binding to the human IL-6 receptor. For human IL-6, it would appear that interactions between residues Ala-180, Leu-181, and Met-184 and residues in the N-terminal region may be critical for maintaining the structure of the molecule; replacement of these residues with the corresponding 3 residues in mouse IL-6 correlated with a significant loss of α-helical content and a 200-fold reduction in activity in the mouse bioassay. A homology model of mIL-6 based on the X-ray structure of human granulocyte colony-stimulating factor is presented.

Keywords: biosensor; CD; chimeras; interleukin-6; molecular modeling; receptor; structure–function

Reprint requests to: Richard J. Simpson, Ludwig Institute for Cancer Research, P.O. Royal Melbourne Hospital., Parkville, Australia 3050; e-mail: simpson@licre.ludwig.edu.au.

[5] Present address: AMRAD Laboratories, Hawthorn, Victoria 3122, Australia.

Abbreviations: EMS, electrospray mass spectrometry; G-CSF, granulocyte colony-stimulating factor; GM-CSF, granulocyte–macrophage colony-stimulating factor; GH, growth hormone; h, human; IL-, interleukin; IL-6, interleukin-6; IL-6R, IL-6 receptor; m, murine; PBS, phosphate-buffered saline; shIL-6R, soluble human IL-6 receptor; RU, resonance units; SCR, structurally conserved region; SPR, surface plasmon resonance.

Interleukin-6 is a multifunctional cytokine that plays an important role in host defense. Its major activities include the ability to induce the growth and differentiation of B lymphocytes, differentiation and/or activation of T lymphocytes and macrophages, expression of acute-phase proteins from the liver, maturation of megakaryocytes, and enhancement of multipotential hematopoietic colony formation (for reviews see Heinrich et al., 1990; Van Snick; 1990; Hirano, 1992; Akira et al., 1993). Dysregulated expression of IL-6 has been observed in autoimmune, chronic proliferative and malignant diseases such as

rheumatoid arthritis, mesangial proliferative glomerulonephritis, plasmacytoma and myeloma, lymphoma, and leukemia (Akira et al; 1993). More recently, IL-6 has been shown to be implicated in bone metabolism (Jilka et al., 1992; Akira et al., 1993; Tamura et al., 1993). A clinical trial in which anti-IL-6 antibodies were used for the therapy of plasma cell leukemia revealed that myeloma cell proliferation could be temporarily blocked with no major side effects to the patient (Klein et al., 1991). Thus, antagonists that inhibit or modulate the action of IL-6 may be of potential therapeutic benefit in IL-6-mediated diseases.

The primary structures of human IL-6 and murine IL-6 consist of 184 and 187 amino acids, respectively, and exhibit 42% amino acid sequence identity (Hirano et al., 1986; Simpson et al., 1988a; Van Snick et al., 1988). Along with a number of other growth factors, which include IL-2, IL-3, IL-4, IL-5, IL-7, granulocyte-macrophage colony-stimulating factor, granulocyte colony-stimulating factor, erythropoietin, leukemia inhibitory factor, and growth hormone, IL-6 belongs to a class of hematopoietins that have been predicted to be 4 α-helical bundle structures (Bazan, 1990, 1991; Parry et al., 1991). High-resolution tertiary structure determinations of a number of these hematopoietins (e.g., GM-CSF, G-CSF, macrophage colony-stimulating factor, IL-2, IL-4, IL-5, and GH) reveal that the above-mentioned cytokines share a common 4-helical bundle up-up-down-down topology (Kaushansky & Karplus, 1993 and references therein; Sprang & Bazan, 1993).

The biological effects of IL-6 on target cells are mediated by 2 transmembrane proteins: the IL-6 receptor, which binds IL-6 (Yamasaki et al., 1988); and gp130 (Taga et al., 1989), which after association with the IL-6/IL-6R complex forms a higher-order complex (Murakami et al., 1993; Ward et al., 1994) and transduces the extracellular signal into the cell (Taga et al., 1989; Hibi et al., 1990). The binding of IL-6 to the IL-6R is species dependent. Whereas hIL-6 binds to both human and murine IL-6R, mIL-6 only binds to the mIL-6R (Coulie et al., 1989). The association of gp130 with the IL-6/IL-6R complex induces high-affinity binding (Hibi et al., 1990) but is not species specific for mouse or human IL-6/IL-6R complexes (Taga et al., 1989; Sugita et al., 1990; Fiorillo et al., 1992b; Saito et al., 1992). Results from IL-6 crosslinking studies on human cells suggest that high-affinity binding involves the binding of hIL-6 to both hIL-6R and gp130 (D'Alessandro et al., 1993).

In view of the potential clinical importance of hIL-6 antagonists, it is of interest to define the region(s) of hIL-6 involved in binding to the hIL-6R. Epitope mapping studies of hIL-6 have shown that neutralizing monoclonal antibodies against hIL-6 were directed toward the N- and C-terminal regions of IL-6, suggesting that these regions are in close proximity (Brakenhoff et al., 1990) and that residues 153–162 are important for biological activity on human cells (Ida et al., 1989). More direct evidence implicating the C-terminal region in receptor binding was obtained by site-directed mutagenesis studies (Nishimura et al., 1991, 1992; Leebeek et al., 1992; Leebeek & Fowlkes, 1992; Yasueda et al., 1992; Li et al., 1993; Savino et al., 1993), from deletion mutants (Krüttgen et al., 1990; Fontaine et al., 1993), and from murine/human IL-6 chimeras (Fiorillo et al., 1992a; Van Dam et al., 1993). By contrast, the N-terminal 28 amino acid residues of hIL-6 can be deleted without loss of biological activity (Brakenhoff et al., 1989). Residues 29–34 have been proposed to participate in the folding of the hIL-6R-binding domain (Brakenhoff et al., 1989; Arcone et al., 1991; Fontaine et al., 1991). There is also evidence that residues 88–105 (Ekida et al., 1992) and 40–96 (Van Dam et al., 1993) of hIL-6 are involved in binding to the hIL-6R.

Recently, we showed, using NMR spectroscopy, that the N- and C-terminii of mIL-6 are in close proximity (Ward et al., 1993). Furthermore, substitution of the 5 C-terminal amino acids of mIL-6 for the corresponding human residues increases the conformational stability of the molecule without affecting its action on murine cells (Ward et al., 1993). In the present investigation, we have taken advantage of the limited species cross reactivity between murine and human IL-6 and generated a series of murine/human IL-6 chimeras to further assess whether the C-terminal residues of hIL-6 are involved in receptor binding and biological activity. The rationale for the design of the chimeras was based on the predicted 4-helical structure of IL-6, as first proposed by Bazan (1990, 1991) and later by Parry and coworkers (1991). Our data imply that 2 regions of hIL-6, the C-terminal residues 178–184 and residues 63–113, are critical for efficient binding to the hIL-6R. We conclude that interactions between residues in the N- and C-terminal regions of hIL-6 are important for maintaining the conformation of the molecule and, therefore, biological activity.

Results

Design of murine/human IL-6 chimeras

The aim of the present investigation was to determine regions of hIL-6 that contribute to binding to hIL-6 receptors. Recognizing the species specificity of human and murine IL-6, a series of murine/human IL-6 chimeras were constructed by recombinant DNA means, in which N- and/or C-terminal regions of mIL-6 were substituted for the corresponding regions in the human molecule. Because the tertiary structure of IL-6 is not known, our rationale for the IL-6 chimeras design was based on the 4 α-helical bundle structure model of Bazan (1991) (Fig. 1).

To introduce restriction endonuclease sites at the intended species crossover points, the cDNAs of h- and mIL-6 were subjected to site-directed mutagenesis in the vector pCDM8. Chimeras M1–M3 (Fig. 2) were then generated by "domain swapping" and subcloning into the bacterial expression vector pUC8. The species crossover points in the connecting loop AB of both M2 and M3 were introduced between the 2 disulfide bonds (Cys_{44}–Cys_{50} and Cys_{73}–Cys_{83} in hIL-6, and correspondingly in mIL-6) (Simpson et al., 1988b; Clogston et al., 1989) at residues Leu-62 (hIL-6) and Lys-65 (mIL-6). The hybrids M4 and M5 (Fig. 2) were generated by PCR using the cDNAs of M1, M2, and hIL-6 as templates. The chimeras M1–M5 contain no internal amino acid deletions or additions but are truncated at their N-terminii (Fig. 2). It has been reported that the N-terminal 28 amino acids of hIL-6 (Brakenhoff et al., 1989) and 22 amino acids of mIL-6 (Ward et al., 1993) can be deleted without loss of biological activity.

Chimera M4 was designed to investigate whether the 7 C-terminal residues of hIL-6, together with the N-terminal region of hIL-6, encompassing helix A and part of the connecting loop AB, would confer hIL-6R binding specificity. We have shown previously that chimera pMC5H (cf. Fig. 2), which comprises mIL-6 with the 7 C-terminal residues substituted with the corresponding residues of hIL-6, is fully active on murine cells, but

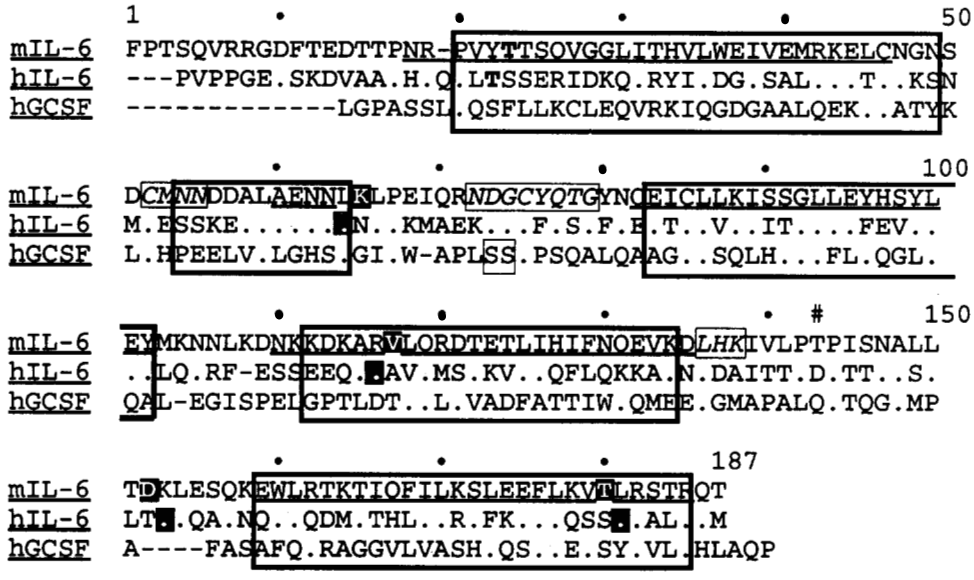

Fig. 1. Amino acid sequence alignment of murine and human IL-6 and hG-CSF. The numbering of residues and position of the O-linked glycosylation site (#) in mIL-6 is from Simpson et al. (1988a); mIL-6 residues 4 and 187 correspond to hIL-6 residues 1 and 184, respectively. The single-letter amino acid code has been used. Gaps in the sequences due to the alignment are represented by (-), residues identical to mIL-6 are shown as (.). The amino acids at the species crossover points of the chimeras M1-M5 and pMC5H are highlighted on a black background. The amino acids shown in bold face indicate the N-terminal residues of the chimeras M1-M5 and pMC5H following the vector-derived sequence. The regions that were originally chosen as structurally conserved regions for the homology modeling of mIL-6 on hG-CSF (see the Materials and methods and Fig. 3) are framed with thick lines; these SCRs comprised helices A, B, C, and D (mIL-6 residues 20–49, 83–102, 112–134, and 159–185, respectively) and residues 54–64 in the AB-loop. A turn observed in the AB-loop of hG-CSF (Hill et al., 1993), but not chosen as SCR, is framed with a thin line. Helical regions and turns of the final mIL-6 homology model are underlined and framed with thin lines, respectively. Helical regions as predicted by Bazan (1991) are mIL-6 residues 21–43 (helix A), 83–105 (helix B), 113–134 (helix C), and 165–187 (helix D).

shows no binding to human cells at concentrations up to 1 μg/mL (Ward et al., 1993). The hybrid M5 was designed to assess whether residues outside the N- and C-terminal regions of hIL-6 contribute to receptor binding interactions.

Homology modeling of mIL-6

The full length primary structures of mIL-6, hIL-6, and hG-CSF, the cytokine with the highest amino acid sequence identity to IL-6 (Bazan, 1991), are aligned in Figure 1, indicating the species crossover points of the chimeras. Using this alignment, a homology model of mIL-6 based on the X-ray structure of hG-CSF (Hill et al., 1993) was constructed (Fig. 3; Kinemage 1). To better illustrate the design of the chimeras, hybrids M3–M5 are superimposed on the homology model of mIL-6 (Fig. 3).

Refinement of our model of mIL-6 resulted in differences in secondary structure compared with hG-CSF in both helical and connecting-loop regions, even though the overall similarity with hG-CSF is maintained. Although both helices B and C are slightly extended in mIL-6, their backbone positions, as well as those of the C-terminal region of helix A and the N-terminal region of helix D, did not change much during refinement and overlay well with the corresponding helices of hG-CSF. Contrary to hG-CSF, helix A in mIL-6 is kinked at Gly-28 and Gly-29, resulting in a slight bending of the N-terminal residues of this helix toward helix D. Thus, the N-terminal region of helix A and C-terminal region of helix D are bent away from the positions of the corresponding regions in hG-CSF by <5 Å and <7 Å, respectively. The helical region identified in the AB-loop of both hG-CSF (Hill et al., 1993) and hGH (de Vos et al., 1992) is shorter in mIL-6 and preceded by a short turn. In contrast with hG-CSF, there also exists an almost helical turn region in the C-terminal part of the AB-loop of mIL-6. This turn is stabilized by a disulfide bridge linking it to helix B. Finally, our model identifies hydrophobic surface patches in the N-terminal part of helix B (residues 86–94) and in the CD-loop (residues 139–150).

Expression, purification, and structural characterization of hIL-6 and murine/human IL-6 chimeras

Human IL-6 and the chimeras M1–M5 and pMC5H were expressed in *Escherichia coli* and purified from "inclusion bodies" to >95% purity, following the protocol previously described for recombinant mIL-6 (Zhang et al., 1992).

The purified products were subjected to N-terminal amino acid sequence analysis and EMS and all but pMC5H were found to contain approximately 15% of material lacking the N-terminal threonine residue (data not shown). The molecular masses of hIL-6 and M1–M5, as determined by EMS, were all within 0.02% of the calculated average molecular masses (data not shown).

To probe the conformational states of the chimeras, the secondary structural contents were determined by far-UV CD (Fig. 4). In all cases, the spectra were characteristic of proteins possessing high contents of α-helix, i.e., minima at 208 nm and 222 nm and a maximum at 193 nm. However, comparison of

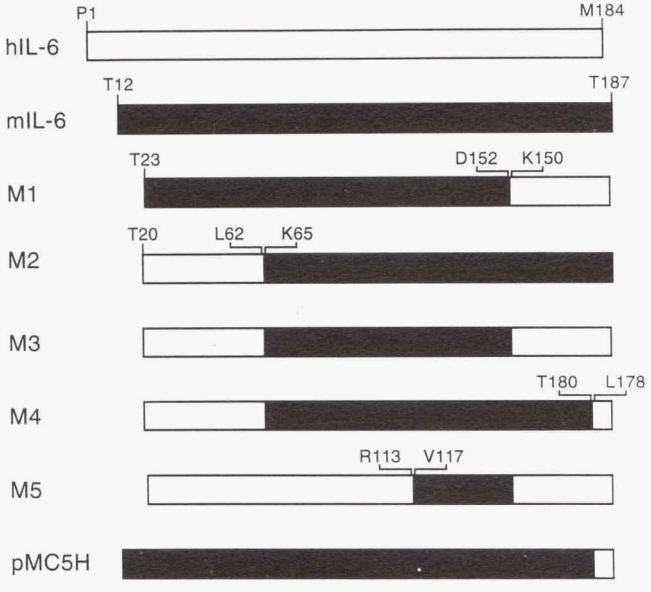

Fig. 2. Schematic representation of IL-6 and murine/human IL-6 chimeras. Alignment of hIL-6 (white) and mIL-6 (black) and the chimeras M1–M5 and pMC5H. The murine and human regions of the IL-6 chimeras are depicted in black and white, respectively. The N- and C-terminal amino acids of each protein or section thereof are given only when differing from previous proteins. The single-letter amino acid code has been used. Amino acids shared between mIL-6 and hIL-6 at species crossover points are counted as human and depicted white. The discontinuous numbering of amino acid residues at species crossover points reflects the difference in length between the mIL-6 and hIL-6 polypeptide chains (187 and 184 residues, respectively). No internal deletions or additions of amino acids have been introduced.

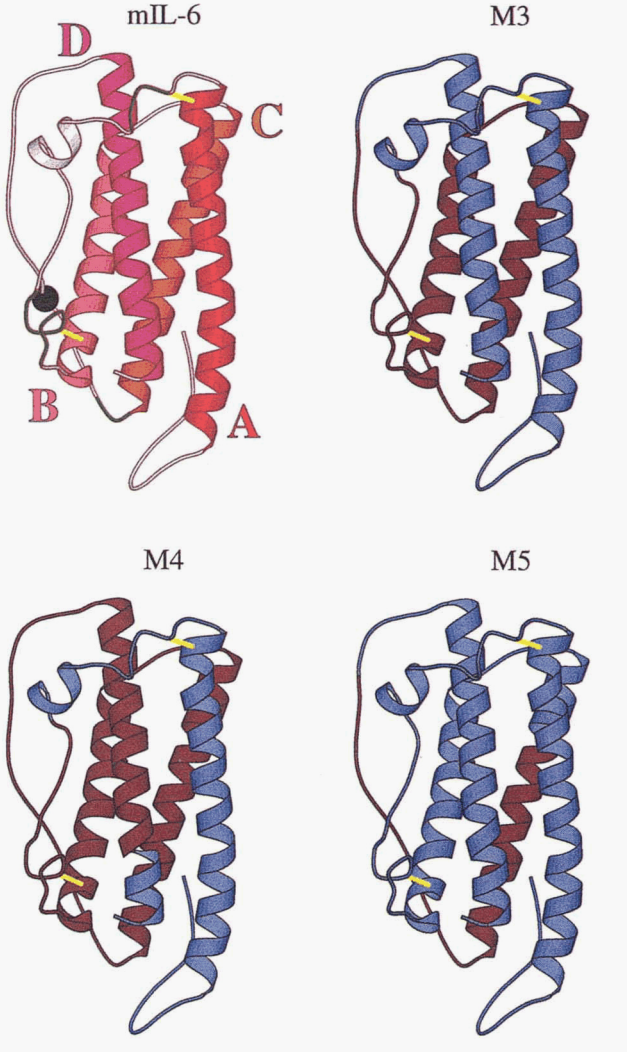

Fig. 3. Homology model of mIL-6 based on human G-CSF. Murine IL-6 was modeled on hG-CSF as described in the Materials and methods, using the alignment shown in Figure 1. The α-helices A, B, C, and D are depicted as colored coiled ribbons, the α-helix in the AB-loop as a white coiled ribbon, the connecting loops as white tubes, and the disulfide bridges as yellow rods. Turns observed in the loop regions are colored green. The black sphere indicates Thr-143, which is glycosylated (Simpson et al., 1988a). The figure was prepared using the program MOLSCRIPT (Kraulis, 1991). Human regions in chimeras M3, M4, and M5 are colored blue on an mIL-6 (red) backbone. The disulfide bridges in the chimeras are depicted as yellow rods.

the spectra of the chimeras with that of hIL-6 revealed small, but significant differences. Whereas the spectrum for M3 was virtually indistinguishable from that of hIL-6, relative decreases in ellipticity at 220 nm of 19, 23, and 15% were calculated for M1, M4, and M5, respectively. The largest change was for M2, with a calculated decrease in ellipticity of 40%.

Mitogenic activity and receptor binding on murine hybridoma cells

The abilities of the chimeras M1–M5 to bind to and activate mIL-6 receptors were assessed using the murine hybridoma cell line 7TD1 (Fig. 5). Murine IL-6 and hIL-6 exerted half-maximal growth stimulation (EC_{50}) at approximately 2 pg/mL and 60 pg/mL, respectively (Fig. 5A). The chimeras M1, M3, and M4 were virtually equipotent with hIL-6 and exerted half-maximal growth stimulation at 7, 13, and 18 pg/mL, respectively. The chimeras M2 and M5 induced half-maximal mitogenic responses at approximately 400 and 1,000 pg/mL, respectively.

The results of experiments measuring competition with ^{125}I-labeled mIL-6 for binding to 7TD1 cells (Fig. 5B) were concordant with the relative potencies of chimeras M1–M5 in the hybridoma growth factor assay. Chimera pMC5H has been shown previously to be approximately equipotent to mIL-6 in both assays on 7TD1 cells (Ward et al., 1993). Taken together, the data show that all of the chimeras were able to bind and activate IL-6 receptors on murine 7TD1 cells.

Competitive receptor binding assay on human myeloma cells

The competition of the IL-6 chimeras with ^{125}I-labeled hIL-6 for binding to receptors on human myeloma U266 cells is shown in Figure 6. The binding of ^{125}I-hIL-6 to the cells was competed for by hIL-6 and M5 with the half-maximal inhibitory concentration (IC_{50}) of M5 being 150 ng/mL, about 9-fold higher than that of hIL-6 (17 ng/mL). The IC_{50} of chimeras M3, M4, and M1 were approximately 6, 10, and 30 μg/mL, respectively. The IC_{50} of pMC5H was extrapolated to be approximately

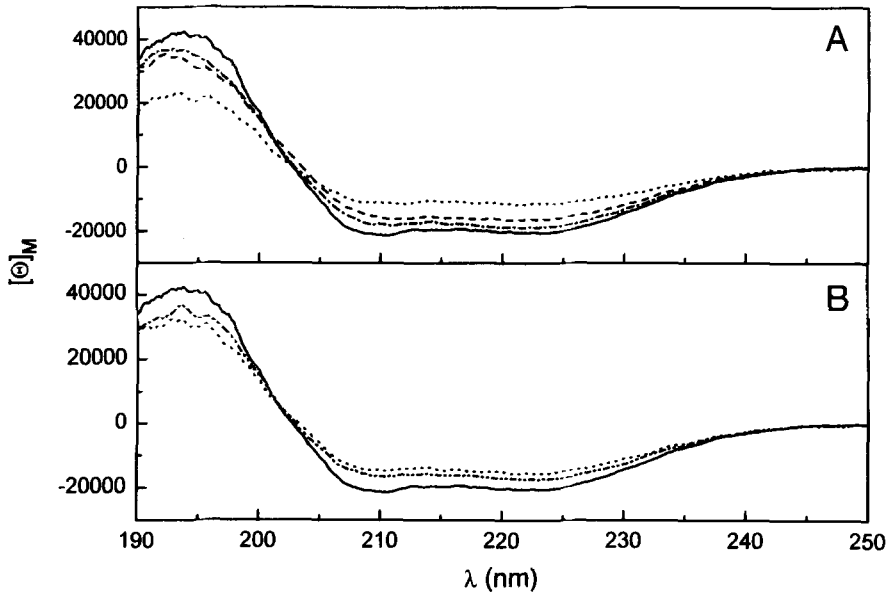

Fig. 4. Far-UV CD spectra of purified murine/human IL-6 chimeras M1–M5. The spectra were recorded at 25 °C, with protein concentrations of 100 μg/mL in 10 mM phosphate buffer, pH 7.4, and expressed as mean residue ellipticity ($[\theta]_{MRW}$). **A:** M1 (– – –), M2 (· · · · ·), M3 (–·–·–), and hIL-6 (——). **B:** M4 (–·–·–), M5 (· · · · ·), and hIL-6 (——).

55 μg/mL. Neither mIL-6 nor M2 showed any significant binding to the U266 cells at 50 μg/mL.

Binding to recombinant soluble hIL-6 receptor

After having established the binding properties of the chimeras to the IL-6R on human cells, we assessed their binding to recombinant soluble hIL-6 receptor by competitive immunoprecipitation assay and biosensor analysis.

Competitive immunoprecipitation assay

Serum R6, a rabbit polyclonal antiserum raised against purified shIL-6R, was used to immunoprecipitate ^{125}I-hIL-6 bound to shIL-6R in the presence of various concentrations of unlabeled competitor. Half-maximal competition was achieved at 20 ng/mL hIL-6 (Fig. 7). Nonspecific binding, defined as bound ^{125}I-hIL-6 in the presence of 500 ng/mL hIL-6, was approximately 5% (data not shown). The chimeras M1, M3–M5, and pMC5H were able to displace ^{125}I-hIL-6, albeit at higher concentrations than hIL-6. Whereas the IC_{50} of M5 and M3 were 200 and 2,200 ng/mL, respectively, the IC_{50} of M1, M4, and pMC5H were 16, 5, and 5 μg/mL. Neither mIL-6 nor M2 competed significantly with ^{125}I-hIL-6 even at 50 μg/mL (Fig. 7).

Biosensor analyses

A biosensor employing SPR detection, (Fägerstam et al., 1992) was also used to analyze the binding of chimeras M1–M5 to shIL-6R. The binding of shIL-6R to immobilized hIL-6 was not prevented by preincubation of shIL-6R (0.5 μg/mL) with M1–M4 at 10 μg/mL in HBS buffer (10 mM *N*-2-hydroxyethyl piperazine-*N*-2-ethane sulfonic acid, pH 7.4, containing 0.15 M NaCl, 3.4 mM ethylenediaminetetraacetic acid, and 0.005% [w/v] Tween-20) containing 0.005% Tween-20 for 1 h at 25 °C (data not shown). Weak binding of M1–M4 could not, however, be discounted because the study of the interactions at high ligand concentrations (~10 μg/mL) was hindered due to nonspecific binding of the chimeras to the sensor surface; treatment of the biosensor chip with 10 mM HCl failed to remove the noncovalently bound material. The nonspecific binding was particularly noticeable for chimera M2.

Using identical conditions as above, significant inhibition of shIL-6R binding to immobilized hIL-6 was observed upon preincubation of shIL-6R with M5 at 10 μg/mL (data not shown). The binding of shIL-6R to M5 was also probed directly by immobilizing M5 to the sensor surface. From the concentration dependence of the equilibrium response, expressed in Scatchard format in Figure 8A, a k_{AX} of 4.76×10^6 M^{-1} (a dissociation equilibrium constant of 210 nM) was calculated. This compares with a k_{AX} of 2.4×10^7 M^{-1} (a dissociation equilibrium constant of 42 nM) for the interaction between shIL-6R and immobilized hIL-6. To exclude the possibility that the immobilization of M5 and hIL-6 through lysine residues had differentially affected their receptor binding properties, the equilibrium constants in solution were determined by competition studies. Data were analyzed by applying expressions developed for quantitative affinity chromatography (Equation 1 in the Materials and methods; Ward et al., 1995). Inhibition of shIL-6R binding to immobilized hIL-6 was obtained after preincubation of shIL-6R with M5 at concentrations up to 100 ng/mL. A K_D of 142 nM was calculated for the interaction in solution of shIL-6R with M5 (Fig. 8B), which compares with a k_{AS} of 5×10^7 M^{-1} (dissociation equilibrium constant of 20 nM) for hIL-6.

In order to differentiate between effects on the association and dissociation rate constants (k_a and k_d, respectively), the kinetics of the binding of shIL-6R to both immobilized M5 and hIL-6 were monitored. Association rate constants of 4.5×10^5 M^{-1} s^{-1} for hIL-6 and 2×10^5 M^{-1} s^{-1} for M5 were calculated (data not shown). The lower affinity of binding to shIL-6R of M5 was, however, largely explained by a more rapid dissociation rate constant. From Figure 8C, values of 0.047 s^{-1} and 0.008 s^{-1} were calculated for the binding of shIL-6R to M5 and hIL-6, respectively.

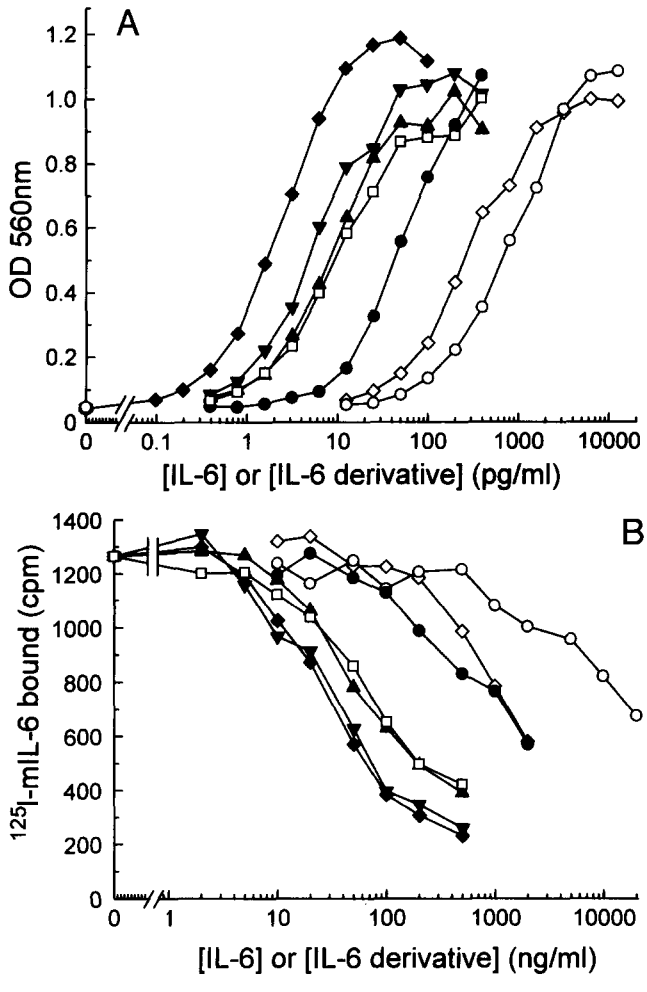

Fig. 5. Biological activity and binding of purified murine/human IL-6 chimeras on mouse hybridoma 7TD1 cells. **A:** Growth-stimulation assay. The 7TD1 cells were incubated with various concentrations of mIL-6 (◆), hIL-6 (●), M1 (▼), M2 (◇), M3 (▲), M4 (□), and M5 (○), as described in the Materials and methods. Mean values of duplicates are plotted. **B:** Competitive binding assay. The 7TD1 cells were incubated on ice for 2 h, in the presence of ^{125}I-labeled mIL-6 and various concentrations of unlabeled competitor as described in the Materials and methods. Symbols are identical to A. Mean values of duplicates are plotted.

Fibrinogen induction from human hepatoma cells

It has been shown that dexamethasone induces IL-6 receptor mRNA expression in HepG2 cells (Heinrich et al., 1990). We found that the addition of 1 μM dexamethasone to the culture medium of human HepG2 cells decreased the background induction of fibrinogen synthesis and increased the stimulation index of hIL-6 (data not shown). The chimeras were therefore assayed in the presence of 1 μM dexamethasone (Fig. 9).

The EC_{50} of hIL-6 on HepG2 cells was approximately 1.5 ng/mL and maximal fibrinogen induction was reached at 12.5 ng/mL hIL-6. Neither mIL-6 nor M2 at concentrations up to 50 μg/mL were able to induce fibrinogen synthesis. Chimeras M1 and pMC5H reached the EC_{50} response of hIL-6 at approximately 3 and 0.78 μg/mL, respectively. Hybrids M3 and M4 elicited a weak response at >2 and >20 μg/mL, respectively, but did not reach the induction level corresponding to the EC_{50} response of hIL-6 (Fig. 9). Chimera M3 was also assayed in the presence of hIL-6 but did not display antagonist activity (data not shown). Chimera M5 had a shallow dose-response curve and reached the EC_{50} response of hIL-6 at approximately 0.15 μg/mL.

Discussion

The functional importance of both the N- and C-terminal regions of IL-6 in the biological activity of this cytokine has been reported by a number of groups (Brakenhoff et al., 1989; Arcone et al., 1991; Lütticken et al., 1991; Fiorillo et al., 1992a; Leebeek et al., 1992; Nishimura et al., 1992; Yasueda et al., 1992; Li et al., 1993; Ward et al., 1993). These studies implicate the involvement of residues in both helices A and D of this predicted 4-helix bundle structure in receptor recognition. However, from these mutation/deletion studies it was not possible to determine whether the N- and C-terminal regions in IL-6 are involved in receptor binding either through direct interaction with the receptor or by stabilizing a binding site elsewhere in the molecule. Brakenhoff et al. (1990) have previously shown by epitope mapping that neutralizing monoclonal antibodies against hIL-6 were directed against regions encompassing both the N- and C-terminus, suggesting that these regions are in close proximity. In a previous study with an mIL-6 variant where the

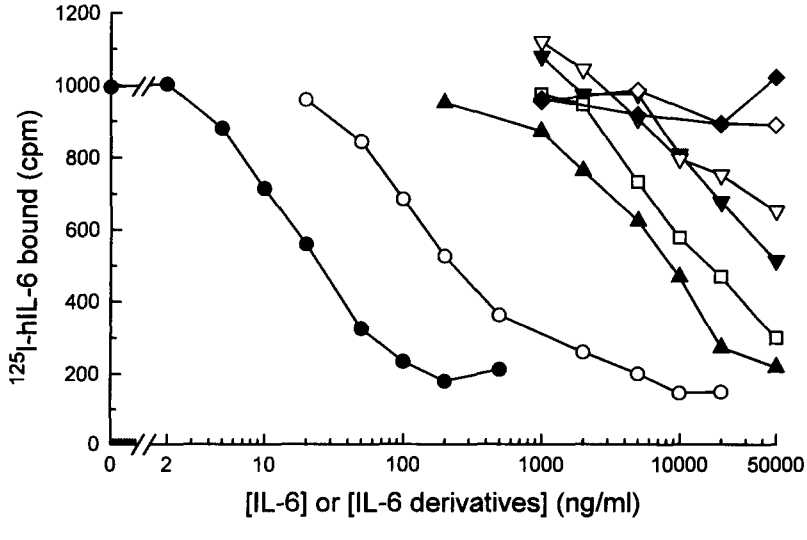

Fig. 6. Receptor binding activity of purified murine/human IL-6 chimeras on human myeloma U266 cells. The U266 cells were incubated on ice for 2 h in the presence of ^{125}I-hIL-6 and various concentrations of hIL-6 (●), M1 (▼), M2 (◇), M3 (▲), M4 (□), M5 (○), pMC5H (▽), or mIL-6 (◆), as described in the Materials and methods. Mean values of duplicates are plotted. The values for mIL-6 and M2 are compiled from 3 different experiments.

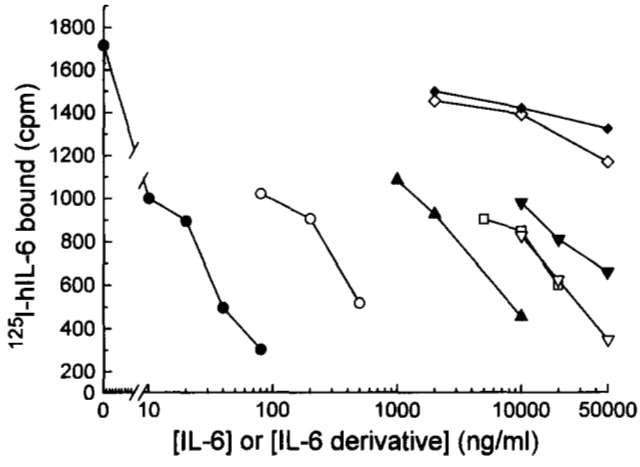

Fig. 7. Receptor binding activity of purified murine/human IL-6 chimeras on soluble human IL-6 receptor. Soluble hIL-6R was incubated at room temperature for 1 h in the presence of ^{125}I-hIL-6 and various concentrations of hIL-6 (●), M1 (▼), M2 (◇), M3 (▲), M4 (□), M5 (○), pMC5H (▽), or mIL-6 (◆). Receptor-bound ^{125}I-hIL-6 was immunoprecipitated with an antiserum specific for shIL-6R, as described in the Materials and methods. Mean values of duplicates are plotted. The values for mIL-6 are compiled from 3 different assays.

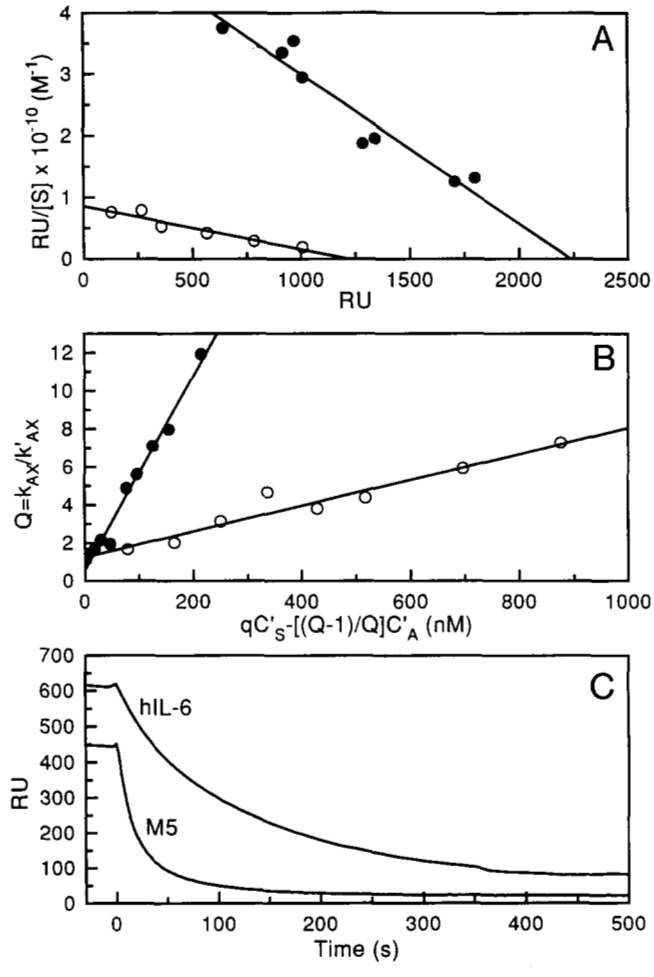

Fig. 8. Binding of purified murine/human chimera M5 to soluble human IL-6 receptor, as monitored by SPR detection. Human IL-6 and chimera M5 were covalently attached to the dextran matrix coating the gold sensor chip as described in the Materials and methods. **A:** Scatchard plot describing equilibrium binding of shIL-6R with immobilized M5 (○) and immobilized hIL-6 (●). **B:** Determination of solution binding constant for the interaction of shIL-6R with M5. Soluble hIL-6R was preincubated with M5 (○) or hIL-6 (●) prior to reaction with immobilized hIL-6. Results are plotted according to Equation 1 in the Materials and methods. **C:** Determination of the dissociation rate constant for the interaction of shIL-6R with immobilized M5 and immobilized hIL-6.

5 C-terminal residues were replaced with the human counterparts, we showed, using NMR, that interactions involving Tyr-22 were influenced by the C-terminal amino acids, suggesting that the N- and C-terminii of mIL-6 are in close proximity (Ward et al., 1993). Equilibrium unfolding experiments in urea indicated that substitution of the 5 C-terminal amino acids of mIL-6 with the corresponding residues from hIL-6 increased the conformational stability of the molecule by 1.4 kcal/mol relative to mIL-6 (Ward et al., 1993).

In the present study we have examined a number of murine/human IL-6 chimeras in order to shed light on the species-specific binding to the hIL-6R. The findings from this study are summarized in Table 1. One of the most salient findings was the observed discrepancy between the mitogenic activities of chimeras M1–M4 and pMC5H on the murine hybridoma cell line 7TD1. Replacement of the C-terminal region (Lys-150 to Thr-187, encompassing helix D and part of the connecting loop CD) of mIL-6 with the corresponding region of hIL-6 (chimera M1) has little effect on activity. However, replacement of the N-terminal region (Thr-20 to Leu-62, encompassing helix A and part of the connecting loop AB) in chimera M2 with the corresponding region of hIL-6 results in a marked (200-fold) decrease in mitogenic activity. These data suggest that, although the N-terminal region of mIL-6 can interact efficiently with the substituted C-terminal region of hIL-6 (chimera M1), or a small portion thereof (7 residues of hIL-6 in the case of chimera pMC5H), the converse interaction (i.e., the N-terminal region of hIL-6 with the C-terminal region of mIL-6, as in chimera M2) does not apply.

CD measurements of the IL-6 chimeras used in this study revealed a significant loss of α-helical content in chimera M2 when compared to chimera M1 and hIL-6 (Fig. 4). Presumably, residues in the N- and C-terminal regions of IL-6 interact to maintain the global fold of the molecule. This finding is in accord with a study by Brakenhoff (1991), which showed that a chimera consisting of the C-terminal 5 mIL-6 residues on an hIL-6 backbone has a 1,000-fold reduced activity on murine B9 cells compared to hIL-6. Interestingly, when one compares chimeras M3 and M4 with M2, restoration of biological activities of M2 can be accomplished by replacing its C-terminal region with the corresponding residues of hIL-6. In fact, replacement of the last 7 C-terminal residues only of chimera M2 (mIL-6 residues 181–187; L R S T R Q T) with the corresponding residues of hIL-6 (resulting in chimera M4) (hIL-6 residues 178–184; L R A L R Q M; cf. Figs. 1, 2) results in marked enhancement of activity (Table 1) and increased α-helical content (Fig. 4). Because 4 of the 7 C-terminal residues are identical in h- and mIL-6 (cf. Fig. 1), it would appear that substitution of residues Ser-183 → Ala, Thr-184 → Leu, and Thr-187 → Met in chimera M2, alone, is sufficient to regain the active structure.

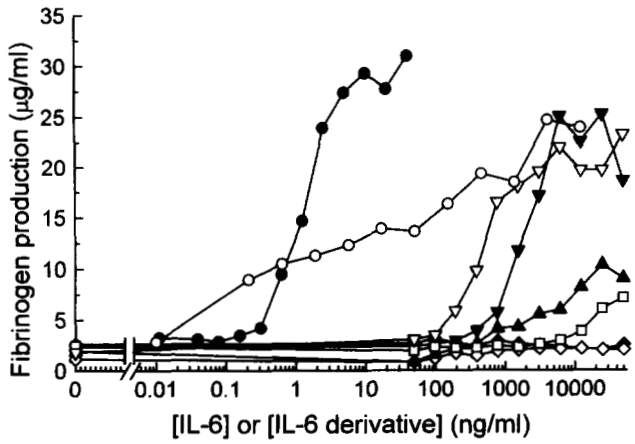

Fig. 9. Activity of purified murine/human IL-6 chimeras in the human HepG2 bioassay. The HepG2 cells were incubated with 1 μM dexamethasone and various concentrations of hIL-6 (●), M1 (▼), M2 (◇), M3 (▲), M4 (□), M5 (○), pMC5H (▽), or mIL-6 (◆). After 6 days, the supernatants were assayed for fibrinogen, as described in the Materials and methods. One representative assay of 3 is shown.

Previous work by Savino et al. (1993) has used saturation mutagenesis in an attempt to identify residues in the C-terminal region of hIL-6 that are critical for binding to the receptor. From these studies it is clear that single-point mutations Ala-180 → Ser and Leu-181 → Thr had little influence on mitogenic activity on mouse hybridoma 7TD1 cells. Other point-mutation work (Lütticken et al., 1991) has shown that hIL-6 with a Met → Thr alteration at position 184 has approximately 50% activity in the murine plasmacytoma B9 proliferation assay compared to hIL-6. Taken together with the result presented in this paper, it appears that alteration of the residues at positions 180, 181, or 184 to the corresponding residues found in mIL-6 has little effect on biological activity. However, if all 3 positions are altered simultaneously there is a drastic loss of activity (compare chimeras M2 and M4). One explanation for the above observations is that the C-terminal region of IL-6 forms an amphipathic helix. Interestingly, residues Ala-180, Leu-181, and Met-184 are on the hydrophobic face of this helix (helix D) when displayed in a helical wheel projection. Although alteration of any one of these residues can be tolerated, alteration of all 3 residues may destabilize the packing of the hydrophobic faces of helices A and D to such an extent that biological activity is drastically reduced. The homology model of mIL-6 (see below) and recent ^{1}H-NMR studies of the solution structure of synthetic peptides corresponding to the C-terminal region of mIL-6 (Morton et al., 1994) lend support to the current model of the IL-6 structure, which consists of a 4-helical bundle with helix D encompassing the C-terminal 20–30 residues.

Despite its advantages, a potential drawback of chimeric analysis occurs when concerted changes to residues involved in complementary interactions take place during the evolutionary divergence of homologous proteins. Indeed, such coupled changes might be disrupted during the construction of interspecies hybrid molecules. For example, the internal packing of human GM-CSF is stabilized by ionic and hydrogen binding interactions of Ser-29, Asp-31, and Lys-107 (Diederichs et al., 1991; Kaushansky & Karplus, 1993), whereas in mouse GM-CSF these residues are replaced by Met-26, Val-28, and Ile-104 and stabilization is achieved by hydrophobic interactions. A full understanding of the nature of the helical packing of mouse and human IL-6 must await the elucidation and analysis of the 3-dimensional structures of these molecules.

The work presented here on the IL-6 chimeras (Table 1) suggests that the 7 C-terminal amino acids of hIL-6 (residues 178–184) are implicated in binding to the hIL-6R. These data are in accordance with other studies (Fiorillo et al., 1992a; Leebeek et al., 1992; Leebeek & Fowlkes, 1992). A particular feature of our results is that chimera M5 has markedly enhanced binding to the hIL-6R and bioactivity in the HepG2 cell line, relative to the other chimeras. These data suggest that part or all of residues 63–113 (encompassing the connecting loop AB through to the beginning of helix C) also contribute to binding to the hIL-6R. Again, our results are in agreement with previous reports

Table 1. *Summary of receptor binding and bioassay data obtained for murine/human IL-6 chimeras*[a]

Sample	Growth stimulation of 7TD1 cells: EC_{50} (pg/mL)	Competition with ^{125}I-hIL-6 for binding to: U266 cells: IC_{50} (ng/mL)	Competition with ^{125}I-hIL-6 for binding to: shIL-6R: IC_{50} (ng/mL)	Fibrinogen induction from HepG2 cells: EC_{50} (ng/mL)
hIL-6	60	17	20	1.5
mIL-6	2	ND[b]	ND	ND
M1	7	30,000	16,000	3,000
M2	400	ND	ND	ND
M3	13	6,000	2,200	>50,000[c]
M4	18	10,000	5,000	>50,000[c]
M5	1,000	150	200	150
pMC5H	2[d]	55,000[e]	5,000[f]	780

[a] Experimental details of the assays are given in the Materials and methods.
[b] ND; not demonstrable at 50 μg/mL.
[c] Extrapolated from Figure 9.
[d] Data from Ward et al. (1993).
[e] Extrapolated from Figure 6.
[f] Extrapolated from Figure 7.

from other groups using a synthetic peptide competitive binding approach (Ekida et al., 1992) and mouse/human IL-6 chimeras (Van Dam et al., 1993), which implicate residues 88–105 and residues 40–96/135–184, respectively, in receptor recognition. Interestingly, these regions encompass binding site I of GH, another member of the hematopoietin cytokine family (de Vos et al., 1992).

The lack of correlation between the binding of chimera M5 to human U266 cells and shIL-6R and its ability to induce fibrinogen synthesis in HepG2 cells is not surprising because the latter assay also involves the gp130 subunit; these data may simply reflect that M5 has lower efficacy to stimulate gp130. In previous epitope mapping studies (Brakenhoff et al., 1990) it has been shown using neutralizing monoclonal antibodies against hIL-6 that there are 2 distinct binding sites on IL-6; presumably, one site for the 80-kDa receptor interaction and another for gp130. Recent mutation work (Brakenhoff et al., 1994) has been able to uncouple receptor binding activity from transduction of the IL-6 signal. By random mutagenesis of residues Gln-152 to Thr-163 (numbering as in Fig. 1) in the predicted helix D of hIL-6, Brakenhoff and colleagues have produced an hIL-6 mutant that antagonizes the activity of hIL-6 on some target cells (e.g., human CESS and HepG2 cells), but not others (e.g., murine B9 cells) (Brakenhoff et al., 1994). It is interesting in the present study that chimera M5 is active on human HepG2 cells, but essentially inactive on mouse 7TD1 cells. Taken together, these observations indicate that it is possible to construct IL-6 mutants that are active on some target cells, but not others. Given the pleiotropy of IL-6 and the wide range of diseases in which IL-6 may be implicated, the above phenomenon may have therapeutic benefits, particularly in situations where it might be desirable to retain some, but not all, IL-6 activities.

The homology model of mIL-6 presented in this report (Figs. 1, 3; Kinemage 1) is based on the crystal structure of hG-CSF (Hill et al., 1993). Several aspects of our model are in agreement with experimental data, for example, the arrangement of the 2 disulfide bonds and the orientation of the glycosylated residue Thr-143 (on the surface of mIL-6 and facing away from the molecule) (Simpson et al., 1988a, 1988b). Both Trp-36 and Trp-160 are surface exposed (data not shown), which would agree with their ready accessibility to chemical modification (Zhang et al., 1993). The N-terminal 22 residues of mIL-6, which are not important for biological activity (Ward et al., 1993), do not show close contacts with residues in other helices. Furthermore, the distances and interactions between Thr-184 and Thr-23 (Table 2) lend support to previous NMR studies concluding that residues in the C-terminal region of mIL-6 come in close proximity to the N-terminal region (Ward et al., 1993).

In the homology model of mIL-6, several interactions between C-terminally located residues and residues in helix B can be detected (Table 2). Although it remains to be determined whether similar interactions occur in hIL-6, these residues localize to the corresponding regions in hIL-6 that we have identified to be important for binding to the hIL-6 receptor (residues 178–184 and

Table 2. *Interactions involving buried residues in helices A and D of mIL-6*

Side chains[a]		Secondary structure[a]		Interaction[b]		
Residue 1	Residue 2	Position 1	Position 2	Hydrogen bond	Energy (kcal/mol)	Distance[c] (Å)
R19	T23	Helix A	Helix A	–	−2.1	2.0
R19	E132	Helix A	Helix C	+	−101.8	1.8
R19	D135	Helix A	CD loop	–	−72.1	2.6
T23	E132	Helix A	Helix C	+	−13.4	1.9
T23	T184	Helix A	Helix D	–	−1.9	3.2
Q26	E132	Helix A	Helix C	+	−21.4	2.1
V27	T184	Helix A	Helix D	–	−1.6	3.4
L30	L125	Helix A	Helix C	–	−2.1	3.7
V34	L173	Helix A	Helix D	–	−1.4	3.9
V34	L177	Helix A	Helix D	–	−1.4	3.8
E37	L118	Helix A	Helix C	–	−4.2	3.6
M41	L170	Helix A	Helix D	–	−1.2	3.8
L45	T163	Helix A	Helix D	–	−1.0	3.3
T163	N54	Helix D	AB loop	+	−10.4	1.9
K164	N54	Helix D	AB loop	+	−23.7	1.7
F176	I89	Helix D	Helix B	–	−2.6	3.2
V179	I89	Helix D	Helix B	–	−1.6	3.9
T180	I89	Helix D	Helix B	–	−1.5	3.5
S183	C85	Helix D	Helix B	–	−2.1	3.4
S183	I89	Helix D	Helix B	–	−1.1	3.9

[a] See Figure 1 (mIL-6 structure).

[b] Hydrogen bonds between side chains were determined using XPLOR (Brünger, 1992) with a distance cutoff of 3 Å between interacting atoms. Energy is defined as the sum of van der Waals and Coulombic interactions. Only interaction energies smaller than −1 kcal/mol are given. In our model, attractive interactions range between the following energies: −113.6 and −40.3 kcal/mol between charged residues, −32.8 and −0.2 kcal/mol between uncharged polar residues, −4.7 and 0.0 kcal/mol between hydrophobic residues.

[c] Defined as the closest distance between interacting residues.

63–113). It is therefore likely that the hIL-6R binding site involves surface-exposed residues in the vicinity of Cys-83 and Ile-87 in hIL-6 (Cys-85 and Ile-89 in mIL-6; cf. Fig. 1 and Table 2). Preliminary data on a murine/human IL-6 chimera, which contains hIL-6 residues 178–184 and 88–96 (residues 90–98 of mIL-6, cf. Fig. 1), suggest that the latter amino acids do not participate in binding to the hIL-6 receptor (A. Hammacher, unpubl.). However, distances between Thr-187 and Tyr-80–Gln-82 in our model are in agreement with the above conclusion (data not shown). Our model also supports the notion that helix A may be of structural importance rather than being involved directly in binding to the IL-6 receptor (Table 2). Several residues in helix A interact with residues in helix C or the CD-loop, which have not previously been implicated in receptor binding. In addition, helix A interacts with helix D mainly through Leu-170, Leu-173, and Leu-177, all of which are identical or conserved between IL-6 species and hG-CSF (cf. Fig. 1), and therefore likely to be of structural importance.

Finally, in the homology model, Thr-163 and Lys-164 in helix D interact closely with Asn-54 (Table 2). In addition, several of the surface-exposed residues from Asn-55 to Asn-63 in the AB-loop also have strong interactions with Glu-155, Thr-163, or Lys-164 (data not shown). Because the latter 3 residues localize to the region corresponding to the presumed gp130 binding-site in hIL-6 (hIL-6 residues Gln-152–Thr-162; numbering as in Fig. 1; Brakenhoff et al., 1994), it is likely that they form part of the gp130 binding-site of mIL-6. Whether the residues in the AB-loop are of structural or functional importance for the gp130 binding site remains to be determined.

Materials and methods

Construction and expression of IL-6

Human IL-6 complementary DNA in a pGEX expression vector (a kind gift of Dr. T. Wilson, Walter and Eliza Hall Institute, Melbourne) was used as a template for the PCR to create a full-length hIL-6 construct subcloned into *Bam*H 1/*Hin*d III-digested pUC8. Murine IL-6, encoded for by the pUC-derived plasmid p9HP1B5B12 (Simpson et al., 1988b), and hIL-6 in pUC8 were expressed in *E. coli* strain NM 522 as fusion proteins. The N-terminal residues of the fusion proteins, Thr-Met-Ile-Thr-Pro-Ser-Leu-Ala in mIL-6 and Thr-Met-Ile-Thr-Asn-Ser-Arg-Gly-Ser in hIL-6, are derived from β-galactosidase and the polylinker of pUC.

Construction and expression of murine/human IL-6 chimeras

An N-terminally truncated form of hIL-6, commencing at Thr-20, was obtained by PCR using full-length hIL-6 in pUC8 as a template, the sense oligonucleotide "oligo A" (5′) CGACGAA TTCCACCTCTTCAGAA, and the antisense oligonucleotide "oligo B" (5′) TTGTCGACGGATCCCTACATTTGCCGA. An N-terminally truncated form of mIL-6 commencing at Thr-23 was obtained by PCR using p9HP1B5B12 as a template, the sense oligonucleotide (5′) CGACGAATTCCACCACTTCACAA, and the antisense oligonucleotide (5′) TAGTCGACGGATCCC TAGGTTTGCCGA. The PCR products were subcloned into pBluescript (Stratagene, La Jolla, California) and excised from pBluescript using PvuII for ligation with BstX1 adapters and subcloning into pCDM8 (Invitrogen Corp., San Diego, California).

In order to make murine/human IL-6 chimeras M1–M3, restriction endonuclease sites for *Hin*d III and *Bfr* 1 were introduced in the pCDM8 inserts at the intended species crossover points, essentially as described elsewhere (Kunkel et al., 1987), using *E. coli* strains BW313 and MC1061/p3 (Invitrogen Corp.) and M13KO7 helper phage (Pharmacia, Uppsala, Sweden). The primers for the site-directed mutagenesis reactions were: (5′) CTGCTGACGAAGCTTCAGGCACAGAACCA (template hIL-6, *Hin*d III site), (5′) GGCAGAAAACAACCTTAAGC TTCCAAAGATGGCT (template hIL-6, *Bfr* 1 site), (5′) CTAA CAGATAAGCTTGAGTCACAGAAGGA (template mIL-6, *Hin*d III site), and (5′) TGCAGAAAACAATCTTAAGCTTC CAGAGATACAA (template mIL-6, *Bfr* 1 site).

Following restriction endonuclease mapping to identify clones containing the desired mutations, the mutants were digested with *Hin*d III or *Bfr* 1, followed by *Eco*R 1 or *Bam*H 1 for subcloning into pUC8. The restriction endonuclease-treated fragments were agarose gel purified, ligated to form chimeras M1, M2, or M3, and subcloned into *Eco*R 1/*Bam*H 1-digested pUC8. The introduced *Hin*d III and *Bfr* 1 sites correspond to species crossover points D152/K150 and L62/K65, respectively, in M1–M5 (Fig. 2).

Chimera M4 was generated in 1 step by PCR, using M2 as template, the sense oligonucleotide "oligo A," and the antisense oligonucleotide for chimera pMC5H ([5′] GGGATCCCTACA TTTGCCGAAGAGCTCTCAAAGTGACTTTTAG). Chimera M5 was generated in 2 steps by PCR, using "oligo A," the internal antisense oligonucleotide (5′) ACAGCTCGAGCTTG TTCCTCACT, and hIL-6 in pUC8 (commencing at Thr-20) as template in the first reaction, and the internal sense oligonucleotide (5′) AAAGCTCGAGTCCTTCAGAGAG, "oligo B," and M1 as template in the second step. The species crossover point R113/V117 in M5 corresponds to an introduced *Xho* 1 site. Following restriction endonuclease treatment and agarose gel purification, the PCR fragments were subcloned into *Eco*R 1/*Bam*H 1-digested pUC8. Chimera pMC5H was generated by PCR and subcloned into pUC9 as described previously (Ward et al., 1993).

Restriction endonucleases were purchased from Boehringer Mannheim (Mannheim, Germany). All constructs were verified by DNA sequencing using an Applied Biosystems model 370A DNA sequencer (Applied Biosystems, Foster City, California). PCR and sequencing reactions were performed on a PCR System 9600 thermal cycler (Perkin Elmer Corp., Norwalk, California) according to manufacturers' instructions.

The chimeras were expressed as fusion proteins with β-galactosidase in *E. coli* strain NM 522. The N-terminal 6 residues of M1–M5 (Thr-Met-Ile-Thr-Asn-Ser) are identical, followed by Thr-23 of mIL-6 (M1) or Thr-20 of hIL-6 (M2–M5) (numbering according to Simpson et al. [1988b]).

Homology modeling of mIL-6

The sequences of murine and human IL-6 and hG-CSF were aligned using a multiple sequence alignment procedure (Hogeweg & Hesper, 1984; Smith, 1986). The resulting alignment was checked manually to improve alignment of observed hydrophobic patterns, e.g., the heptad repeat motif observed in helices of cytokines (Parry et al., 1991). Our alignment is virtually iden-

tical to Bazan's alignment that best agrees with the distribution of hydrophobic and hydrophilic residues in the interior and exterior surfaces of proteins, respectively (Bazan, 1991); the difference consists of the location of the gaps introduced in hIL-6 and hG-CSF in the sequences corresponding to mIL-6 residues 103–109 (Fig. 1) (cf. Bazan, 1991).

Using the Homology module of Insight II software (BIOSYM Technologies Inc., San Diego, California), an initial model of mIL-6 was built as follows. As part of the fundamental 4-helical bundle cytokine fold (Sprang & Bazan, 1993) the 4 helices A, B, C, and D of mIL-6 were each set as a structurally conserved region. As both hG-CSF (Hill et al., 1993) and hGH (de Vos et al., 1992) have a small helix in the N-terminal region of the connecting AB-loop, and hG-CSF, and IL-6 have an analogous disulfide bridge in this region, residues 54–64 in the AB-loop of mIL-6 were selected as an SCR. Coordinates of mIL-6 SCRs were obtained by replacing side chains of the hG-CSF primary structure with mIL-6 residues according to the alignment shown in Figure 1. Coordinates for atoms in loop regions between SCRs were obtained using loop structures with suitable lengths from the Brookhaven Protein Data Bank (Bernstein et al., 1977). Amino- and carboxyl-terminal regions were built in extended conformations. An alternative model was also built using a different alignment of the D-helices of mIL-6 and hG-CSF. In this alignment, the C-terminal hG-CSF residues A, Q, and P were aligned with mIL-6 residues R185, Q186, and T187, respectively, resulting in the gap in the CD-loop of hG-CSF being shortened by 3 residues (cf. Fig. 1). Although the quality of this alignment was comparable to the original alignment, the resulting model was discarded on the basis of showing a significantly increased number of hydrophobic surface residues.

The model was refined in 3 stages, using simulated annealing procedures similar to the ones described for the construction of a model for human leukemia inhibitory factor (Smith et al., 1994). However, in order to speed up the calculations, the first stages of the refinement were performed in vacuum. Only for the last stage, during 175 ps of unrestrained molecular dynamics calculations, a 5-Å layer of water molecules was created to surround mIL-6. The protein was stable during the last 50 ps of the last refinement step. All refinement steps were performed using the program X-PLOR (Brünger, 1992) in conjunction with the CSDX force field (Engh & Huber, 1991). The stereochemical properties were checked with PROCHECK (Laskowski et al., 1993). The quality of the structure after refinement corresponds to an X-ray structure of 1.5–2.5 Å resolution. The hydropathy pattern of our model is consistent with the core of the protein consisting of hydrophobic residues and the solvent-exposed surface being formed mainly by hydrophilic residues.

Purification of IL-6 and IL-6 chimeras expressed in E. coli

The expression and purification of IL-6 and the chimeras was performed essentially as described for mIL-6 (Zhang et al., 1992), except that L-broth was substituted for 2xTY-broth for the induction of the proteins. Typically, the yield of purified sample exceeded 3 mg/L of isopropyl-1-thio-β-D-galactoside-induced bacterial culture. The purity of the samples was confirmed by N-terminal amino acid sequence analysis and EMS, as described (Ward et al., 1993).

Purification of soluble hIL-6 receptor

The cDNA for shIL-6R (truncated at amino acid residue 344) was expressed in CHO cells as described (Yasukawa et al., 1990). Purification of shIL-6R from culture supernatants was accomplished using an (N63K)hIL-6 affinity column followed by reversed-phase HPLC and size-exclusion chromatography (Ward et al., 1994b).

Protein estimation

The concentrations of IL-6 and shIL-6R were determined by amino acid analysis on a Beckman 6300 Amino Acid Analyzer (Beckman Instruments Inc., Palo Alto, California). The concentrations of the chimeras were calculated from the absorbances at 280 nm in 6 M guanidine-hydrochloride as described (Gill & von Hippel, 1989). The 2 methods of protein estimation yielded values within ±5% of each other.

Far UV CD analysis

Far-UV CD spectra were measured in duplicate at room temperature using an Aviv 62DS CD spectrometer, a 0.1-cm-pathlength cell, a band width of 0.8 nm, a step size of 0.2 nm, and an averaging time of 1 s per step. Reported spectra, calculated using mean residue weights of 115.8, 116.4, 116.3, 116.6, 115.7, and 113.2 for chimeras M1–M5 and hIL-6, respectively, are expressed as mean residue ellipticity $[\theta]_{MRW}$.

Radiolabeling of IL-6

Human IL-6 was labeled with ^{125}I according to the method of Bolton and Hunter (1973) and ^{125}I-mIL-6 was prepared using the chloramine T procedure (Greenwood et al., 1963). Radiolabeled protein was separated from free iodine as described (Nicola & Metcalf, 1984).

Receptor binding assays

Competitive binding studies on the murine hybridoma cell line 7TD1 and the human myeloma cell line U266 were performed essentially as described (Coulie et al., 1989; Ward et al., 1993). Cells were washed and resuspended in binding medium (modified RPMI-1640 medium containing 1% newborn calf serum) before addition of ^{125}I-labeled ligand (approximately 20,000 cpm) and various amounts of unlabeled competitor, in total volumes of 100 μL. The samples were incubated for 2 h on ice prior to transfer to 400-μL centrifuge tubes (Elkay, Shrewsburg, Massachusetts) containing 180 μL newborn calf serum. After a brief centrifugation in an Eppendorf benchtop centrifuge, the tips of the tubes, containing the cell pellets, were cut off and the ^{125}I-IL-6 radioactivity bound was measured in a Packard Multi-Prias gamma counter (Packard Instruments, Downers Grove, Illinois).

Hybridoma growth factor assay

The growth stimulation assay on murine 7TD1 cells was performed essentially as described previously (Van Snick et al., 1986; Ward et al., 1993). Cell growth was determined by assaying succinic dehydrogenase levels using 3-(4,5-dimethylthiazol-

2-yl)-2,5-diphenyltetrazolium bromide as substrate, as described elsewhere (Mosmann, 1983).

Hepatocyte stimulation assay

Human hepatoma HepG2 cells were plated in 96-well flat-bottomed microtiter plates (NUNC, Roskilde, Denmark) (30,000 cells per microwell in a volume of 200 μL) and grown overnight in RPMI supplemented with 20 mM *N*-2-hydroxyethyl piperazine *N*-2-ethane sulfonic acid (BDH Chemicals Australia Pty. Ltd.), streptomycin (12.6 mg/L), penicillin (60 mg/L), and 10% heat-inactivated fetal calf serum at 37 °C and 5% CO_2. Following removal of the spent culture medium, triplicates of test samples were added (in RPMI supplemented as above but with 5% fetal calf serum and 1 μM dexamethasone [David Bull Laboratories, Melbourne, Australia]) for a further incubation of 6 days. The conditioned media of the pooled triplicate samples were assayed in a sandwich ELISA specific for human fibrinogen, using MAX-ISORP-immunoplates (NUNC), rabbit-anti-human fibrinogen antibody (DAKO A/S, Glostrup, Denmark), peroxidase-conjugated rabbit-anti-human-fibrinogen antibody (DAKOPATTS A/S), and TMB Microwell Peroxidase Substrate System (Kirkegaard & Perry Laboratories, Gaithersburg, Maryland). Optical density at 450 nm and 620 nm was measured on a Titertek Multiskan MCC/340 instrument (Labsystems, Helsinki, Finland).

Antisoluble hIL-6R antiserum

Soluble hIL-6R antiserum R6 was obtained after intramuscular injection in rabbit of purified shIL-6R in an emulsion with the adjuvant Hunter's TiterMax (CytRx Corp., Norcross, Georgia).

Analysis of binding to shIL-6R: Immunoprecipitation assay

Soluble hIL-6R (50 ng) was allowed to react for 1 h at room temperature with approximately 25,000 cpm of ^{125}I-labeled hIL-6 and various amounts of unlabeled competitor in PBS containing 0.01% (w/v) Tween-20 (Pierce, Rockford, Illinois) and 2 mg/mL bovine serum albumin (Sigma, Castle Hill, NSW, Australia), in a total volume of 50 μL. Anti-shIL-6R serum R6 (0.5 μL/sample) was then added for 2 h incubation on ice, followed by protein A Sepharose (20 μL packed beads) (Pharmacia, Uppsala, Sweden) and a further incubation of 30 min on ice. Immunoprecipitates were washed 3 times in PBS containing 1% (w/v) Triton X100 (Boehringer Mannheim) and 0.01% Tween 20, prior to counting immunoprecipitated (shIL-6R-bound) ^{125}I-hIL-6 in a Packard Multi-Prias γ-counter.

Ligand-receptor interaction analysis

Binding of ligand to shIL-6R was measured in vitro using a BIAcore™ instrument employing SPR detection (Pharmacia Biosensor, Uppsala, Sweden). Ligand (hIL-6 or M5) was covalently coupled to the carboxylated dextran coating the sensor chip using the *N*-ethyl-N^1-(3-diethylaminopropyl) carbodiimide/*N*-hydroxy succinimide coupling chemistry (Johnsson et al., 1991), as previously described for hIL-6 (Ward et al., 1993). Noncovalently bound ligand was removed by treatment of the surface with 6 M guanidine-hydrochloride for 3 min. Human IL-6 and M5 were derivatized to surface concentrations of 3 ng/mm^2 and 3.9 ng/mm^2, respectively, assuming 1 ng/mm^2 of protein corresponds to a signal of 1,000 RU (Stenberg et al., 1991). The sensor surface was regenerated between assays by treatment with 10 mM HCl for 3 min.

The binding of shIL-6R to immobilized ligand was measured upon introduction of various concentrations of shIL-6R (35 μL) in HBS buffer at a flow rate of 1 μL/min. The association equilibrium constant describing the interaction of shIL-6R with immobilized ligand (k_{AX}) was calculated from the dependence of the equilibrium response (R_P) upon the concentration of applied shIL-6R (C'_A), according to the Scatchard relationship (Scatchard, 1949). The association equilibrium constant for the interaction between ligand and receptor in solution (k_{AS}) was obtained from competition experiments, as described (Ward et al., 1995). The value for k_{AS} was obtained from the slope of a plot of Q versus $C'_S - [(Q - 1)/Q]C'_A$ (Equation 1), where $Q = k_{AX}/k'_{AX}$, k'_{AX} is the constitutive binding constant measured in the presence of competing ligand, and C'_S is the total concentration of competing ligand (Ward et al., 1995).

The association and dissociation rate constants describing the binding of shIL-6R to either immobilized M5 or immobilized hIL-6 were calculated assuming a single class of binding sites using the integrated form of the rate equations as described (O'Shannessy et al., 1993). Nonlinear regression analysis was performed using the Sigmaplot program, which employs the Levenberg-Marquardt algorithm (Marquardt, 1963) for iterative curve fitting.

Acknowledgments

We are grateful to Robert Moritz and Josie Discolo for the purification of the IL-6 mutants, to Gavin Reid for the synthesis of oligonucleotides and mass spectrometric analyses, and to Tu Guo-Fen for DNA sequence analysis of the constructs. We thank Drs. Darryl Maher, Margaret Hibbs, and Steven Stacker for helpful discussions and Dr. A.W. Burgess for critical review of the manuscript. This work was supported by grant 920528 from the National Health and Medical Research Council of Australia and, in part (H.T.), by the Australian Government Cooperative Research Centres Scheme.

References

Akira S, Taga T, Kishimoto T. 1993. Interleukin-6 in biology and medicine. *Adv Immunol 54*:1-78.

Arcone R, Fontaine V, Coto I, Content J, Ciliberto G. 1991. Internal deletions of amino acids 29-42 of human interleukin-6 (IL-6) differentially affect bioactivity and folding. *FEBS Lett 288*:197-200.

Bazan JF. 1990. Haemopoietic receptors and helical cytokines. *Immunol Today 11*:350-354.

Bazan JF. 1991. Neuropoietic cytokines in the hematopoietic fold. *Neuron 7*:197-208.

Bernstein FC, Koetzle TF, Williams GJB, Meyer EF Jr, Brice MD, Rodgers JR, Kennard O, Shimanouchi T, Tasumi M. 1977. The Protein Data Bank: A computer-based archival file for macromolecular structures. *J Mol Biol 112*:535-542.

Bolton AE, Hunter WM. 1973. The labelling of proteins to high specific radioactivities by conjugation to a ^{125}I-containing acylating agent. Application to the radioimmunoassay. *Biochem J 133*:529-539.

Brakenhoff JPJ. 1991. Molecular cloning and structure-function analysis of human interleukin-6 [thesis]. Amsterdam, The Netherlands: University of Amsterdam.

Brakenhoff JPJ, de Hon FD, Fontaine V, ten Boekel E, Schooltink H, Rose-John S, Heinrich PC, Content J, Aarden LA. 1994. Development of a human interleukin-6 receptor antagonist. *J Biol Chem 269*:86-93.

Brakenhoff JPJ, Hart M, Aarden LA. 1989. Analysis of human IL-6 mutants expressed in *Escherichia coli*. Biologic activities are not affected by deletion of amino acids 1–28. *J Immunol 143*:1175–1182.

Brakenhoff JPJ, Hart M, de Groot ER, Di Padova F, Aarden LA. 1990. Structure–function analysis of human IL-6. Epitope mapping of neutralizing monoclonal antibodies with amino- and carboxyl-terminal deletion mutants. *J Immunol 145*:561–568.

Brünger AT. 1992. *X-PLOR, a system for crystallography and NMR (version 3.1)*. Yale University Press, New Haven and London.

Clogston CL, Boone TC, Crandall C, Mendiaz EA, Lu HS. 1989. Disulfide structures of human interleukin-6 are similar to those of human granulocyte colony stimulating factor. *Arch Biochem Biophys 272*:144–151.

Coulie PG, Stevens M, van Snick J. 1989. High- and low-affinity receptors for murine interleukin 6. Distinct distribution on B and T cells. *Eur J Immunol 19*:2107–2114.

D'Alessandro F, Colamonici O, Nordan RP. 1993. Direct association of interleukin-6 with a 130-kDa component of the interleukin-6 receptor system. *J Biol Chem 268*:2149–2153.

de Vos AM, Ultsch M, Kossiakoff AA. 1992. Human growth hormone and extracellular domain of its receptor: Crystal structure of the complex. *Science 255*:306–312.

Diederichs K, Boon T, Karplus PA. 1991. Novel fold and putative receptor binding site of granulocyte–macrophage colony-stimulating factor. *Science 254*:1779–1782

Ekida T, Nishimura C, Masuda S, Itoh SI, Shimada I, Arata Y. 1992. A receptor-binding peptide from human interleukin-6: Isolation and a proton nuclear magnetic resonance study. *Biochem Biophys Res Commun 189*:211–220.

Engh RA, Huber R. 1991. Accurate bond and angle parameters for X-ray protein-structure refinement. *Acta Crystallogr A 47*:392–400.

Fägerstam LG, Frostell-Karlsson A, Karlsson R, Persson B, Rönnberg I. 1992. Biospecific interaction analysis using surface plasmon resonance detection applied to kinetic, binding site and concentration analysis. *J Chromatogr 597*:397–410.

Fiorillo MT, Cabibbo A, Iacopetti P, Fattori E, Ciliberto G. 1992a. Analysis of human/mouse interleukin-6 hybrid proteins: Both amino- and carboxy termini of human interleukin-6 are required for in vitro receptor binding. *Eur J Immunol 22*:2609–2615.

Fiorillo MT, Toniatti C, van Snick J, Ciliberto G. 1992b. Expression of the murine interleukin 6 receptor in hepatoma cells: The intracytoplasmic domain is not required for interleukin 6 signal transduction. *Eur J Immunol 22*:799–804.

Fontaine V, Brakenhoff J, de Wit L, Arcone R, Ciliberto G, Content J. 1991. Internal deletions in human interleukin-6: Structure–function analysis. *Gene 104*:227–234.

Fontaine V, Savino R, Arcone R, de Wit L, Brakenhoff JPJ, Content J, Ciliberto G. 1993. Involvement of the Arg 179 in the active site of human IL-6. *Eur J Biochem 211*:749–755.

Gill SC, von Hippel PH. 1989. Calculation of protein extinction coefficients from amino acid sequence data. *Anal Biochem 182*:319–326.

Greenwood FC, Hunter WM, Glover JS. 1963. The preparation of ^{131}I-labelled human growth hormone of high specific radioactivity. *Biochem J 89*:114–123.

Heinrich PC, Castell JV, Andus T. 1990. Interleukin-6 and the acute phase response. *Biochem J 265*:621–636.

Hibi M, Murakami M, Saito M, Hirano T, Taga T, Kishimoto T. 1990. Molecular cloning and expression of an IL-6 signal transducer, gp130. *Cell 63*:1149–1157.

Hill CP, Osslund TD, Eisenberg D. 1993. The structure of granulocyte-colony-stimulating factor and its relationship to other growth factors. *Proc Natl Acad Sci USA 90*:5167–5171.

Hirano T. 1992. The biology of interleukin-6. In: Kishimoto T, ed. *Interleukins: Molecular biology and immunology, Chem Immunol 51*. Basel: Karger. pp 153–180.

Hirano T, Yasukawa K, Harada H, Taga T, Watanabe Y, Matsuda T, Kashiwamura SI, Nakajima K, Koyama K, Iwamatsu A, Tsunasawa S, Sakiyama F, Matsui H, Takahara Y, Taniguchi T, Kishimoto T. 1986. Complementary DNA for a novel human interleukin (BSF-2) that induces B lymphocytes to produce immunoglobulin. *Nature 324*:73–76.

Hogeweg P, Hesper B. 1984. The alignment of sets of sequences and the construction of phyletic trees: An integrated method. *J Mol Evol 20*:175–186.

Ida N, Sakurai S, Hosaka T, Hosoi K, Kunitomo T, Shimazu T, Maruyama T, Matsuura Y, Kohase M. 1989. Establishment of strongly neutralizing monoclonal antibody to human interleukin-6 and its epitope analysis. *Biochem Biophys Res Commun 165*:728–734.

Jilka RL, Hangoc G, Girasole G, Passeri G, Williams DC, Abrams JS, Boyce B, Broxmeyer H, Manolagas SC. 1992. Increased osteoclast development after estrogen loss: Mediation by interleukin-6. *Science 257*:88–91.

Johnsson B, Löfås S, Lindquist G. 1991. Immobilization of proteins to a carboxymethyldextran-modified gold surface for biospecific interaction analysis in surface plasmon resonance sensors. *Anal Biochem 198*:268–277.

Kaushansky K, Karplus PA. 1993. Hematopoietic growth factors: Understanding functional diversity in structure terms. *Blood 82*:3229–3240.

Klein B, Wijdenes J, Zhang XG, Jourdan M, Boiron JM, Brochier J, Liautard J, Merlin M, Clement C, Morel-Fournier B, Lu ZY, Mannoni P, Sany J, Bataille R. 1991. Murine anti-interleukin-6 monoclonal antibody therapy for a patient with plasma cell leukemia. *Blood 78*:1198–1204.

Kraulis PJ. 1991. MOLSCRIPT: A program to produce both detailed and schematic plots of protein structures. *J Appl Crystallogr 24*:946–950.

Krüttgen A, Rose-John S, Dufhues G, Bender S, Lütticken C, Freyer P, Heinrich PC. 1990. The three carboxy-terminal amino acids of human interleukin-6 are essential for its biological activity. *FEBS Lett 273*:95–98.

Kunkel TA, Roberts JD, Zakour RA. 1987. Rapid and efficient site-specific mutagenesis without phenotypic selection. *Methods Enzymol 154*:367–382.

Laskowski RA, MacArthur MW, Moss DS, Thornton JM. 1993. PROCHECK: A program to check the stereochemical quality of protein structures. *J Appl Crystallogr 24*:946–950.

Leebeek FWG, Fowlkes DM. 1992. Construction and functional analysis of hybrid interleukin-6 variants. Characterization of the role of the C-terminus for species specificity. *FEBS Lett 306*:262–264.

Leebeek FWG, Kariya K, Schwabe M, Fowlkes DM. 1992. Identification of a receptor binding site in the carboxyl terminus of human interleukin-6. *J Biol Chem 267*:14832–14838.

Li X, Rock F, Chong P, Cockle S, Keating A, Ziltener H, Klein M. 1993. Structure–function analysis of the C-terminal segment of human interleukin-6. *J Biol Chem 268*:22377–22384.

Lütticken G, Krüttgen A, Möller C, Heinrich PC, Rose-John S. 1991. Evidence for the importance of a positive charge and an α-helical structure of the C-terminus of biological activity of human IL-6. *FEBS Lett 282*: 265–267.

Marquardt DW. 1963. An algorithm for least-squares estimation of non-linear parameters. *J Soc Ind Appl Math 11*:431–441.

Morton CJ, Simpson RJ, Norton RS. 1994. ^{1}H-NMR study of the solution structure of synthetic peptides corresponding to the C-terminal helix of interleukin-6. *Eur J Biochem 219*:97–107.

Mosmann T. 1983. Rapid colorimetric assay for cellular growth and survival: Application to proliferation and cytotoxicity assays. *J Immunol Methods 65*:55–63.

Murakami M, Hibi M, Nakagawa N, Nakagawa T, Yasukawa K, Yamanishi K, Taga T, Kishimoto T. 1993. IL-6-induced homodimerization of gp130 and associated activation of a tyrosine kinase. *Science 260*:1808–1810.

Nicola NA, Metcalf D. 1984. Binding of the differentiation-inducer, granulocyte-colony-stimulating factor, to responsive but not unresponsive leukemic cell lines. *Proc Natl Acad Sci USA 81*:3765–3769.

Nishimura C, Ekida T, Nomura K, Sakamoto K, Suzuki H, Yasukawa K, Kishimoto T, Arata Y. 1992. Role of leucine residues in the C-terminal region of human interleukin-6 in the biological activity. *FEBS Lett 311*:271–275.

Nishimura C, Futatsugi K, Yasukawa K, Kishimoto T, Arata Y. 1991. Site-specific mutagenesis of human interleukin-6 and its biological activity. *FEBS Lett 281*:167–169.

O'Shannessy DJ, Brigham-Burke M, Soneson KK, Hensley P, Brooks I. 1993. Determination of rate and equilibrium binding constants for macromolecular interactions using surface plasmon resonance: Use of nonlinear least squares analysis methods. *Anal Biochem 212*:457–468.

Parry DAD, Minasian E, Leach SJ. 1991. Cytokine conformations: Predictive studies. *J Mol Recognition 4*:63–75.

Saito M, Yoshida K, Hibi M, Taga T, Kishimoto T. 1992. Molecular cloning of a murine IL-6 receptor-associated signal transducer, gp130, and its regulated expression in vivo. *J Immunol 148*:4066–4071.

Savino R, Lahm A, Giorgio M, Cabibbo A, Tramontano A, Ciliberto G. 1993. Saturation mutagenesis of the human interleukin 6 receptor-binding site: Implications for its three dimensional structure. *Proc Natl Acad Sci USA 90*:4067–4071.

Scatchard G. 1949. The attractions of proteins for small molecules and ions. *Ann NY Acad Sci 51*:660–669.

Simpson RJ, Moritz RL, Rubira ML, van Snick J. 1988a. Murine hybridoma/plasmacytoma growth factor. Complete amino-acid sequence and relation to human interleukin-6. *Eur J Biochem 176*:187–197.

Simpson RJ, Moritz RL, van Roost E, van Snick J. 1988b. Characterization of a recombinant murine interleukin-6: Assignment of disulfide bonds. *Biochem Biophys Res Commun 157*:364–372.

Smith DK. 1986. The alignment of macromolecular sequences [thesis]. Canberra, Australia: University of Canberra, ACT.

Smith DK, Treutlein HR, Maurer T, Owczarek CM, Layton MJ, Nicola NA, Norton RS. 1994. Homology modelling and ^{1}H NMR studies of human leukemia inhibitory factor. *FEBS Lett 350*:275–280.

Sprang SR, Bazan JF. 1993. Cytokine structural taxonomy and mechanisms of receptor engagement. *Curr Opin Struct Biol 3*:815–827.

Stenberg E, Persson B, Roos H, Urbaniczky C. 1991. Quantitative determination of surface concentration of protein with surface plasmon resonance using radiolabeled proteins. *J Colloid Interface Sci 143*:513–526.

Sugita T, Totsuka T, Saito M, Yamasaki K, Taga T, Hirano T, Kishimoto T. 1990. Functional murine interleukin 6 receptor with the intracisternal A particle gene product at its cytoplasmic domain. *J Exp Med 171*:2001–2009.

Taga T, Hibi M, Hirata Y, Yamasaki K, Yasukawa K, Matsuda T, Hirano T, Kishimoto T. 1989. Interleukin-6 triggers the association of its receptor with a possible signal transducer, gp130. *Cell 58*:573–581.

Tamura T, Udagawa N, Takahashi N, Miyaura C, Tanaka S, Yamada Y, Koishihara Y, Ohsugi Y, Kumaki K, Taga T, Kishimoto T, Suda T. 1993. Soluble interleukin-6 receptor triggers osteoclast formation by interleukin-6. *Proc Natl Acad Sci USA 90*:11924–11928.

Van Dam M, Mullberg J, Schooltink H, Stoyan T, Brakenhoff JPJ, Graeve L, Heinrich PC, Rose-John S. 1993. Structure-function analysis of interleukin-6 utilizing human/murine chimeric molecules. Involvement of two separate domains in receptor binding. *J Biol Chem 268*:15285–15290.

Van Snick J. 1990. Interleukin-6: An overview. *Annu Rev Immunol 8*:253–278.

Van Snick J, Cayphas S, Szikora JP, Renauld JC, Van Roost E, Boon T, Simpson RJ. 1988. cDNA cloning of murine interleukin-HP-1: Homology with human interleukin-6. *Eur J Immunol 18*:193–198.

Van Snick J, Cayphas S, Vink A, Uyttenhove C, Coulie P, Rubira MR, Simpson RJ. 1986. Purification and NH_2-terminal amino acid sequence of a T-cell-derived lymphokine with growth factor activity for B-cell hybridomas. *Proc Natl Acad Sci USA 83*:9679–9683.

Ward LD, Hammacher A, Chang J, Zhang JG, Discolo G, Moritz RL, Yasukawa K, Simpson RJ. 1994b. Reconstitution in vitro of the interleukin-6/interleukin-6 receptor interaction: Direct monitoring using a biosensor employing surface plasmon resonance detection. In: Crabb JW, ed. *Techniques in protein chemistry V*. New York: Academic Press. pp 331–338.

Ward LD, Hammacher A, Zhang JG, Weinstock J, Yasukawa K, Morton CJ, Norton RS, Simpson RJ. 1993. Role of the C-terminus in the activity, conformation and stability of interleukin-6. *Protein Sci 2*:1472–1481.

Ward LD, Howlett GJ, Discolo G, Yasukawa K, Hammacher A, Moritz RL, Simpson RJ. 1994a. The high affinity interleukin-6 (IL-6) receptor is a hexameric complex consisting of two molecules of each IL-6, IL-6 receptor and gp-130. *J Biol Chem 269*:23286–23289.

Ward LD, Howlett GJ, Hammacher A, Weinstock J, Yasukawa K, Simpson RJ, Winzor DJ. 1995. Use of a biosensor with surface plasmon resonance detection for the determination of binding constants: Measurement of interleukin-6 binding to the soluble interleukin-6 receptor. *Biochemistry*. Forthcoming.

Yamasaki K, Taga T, Hirata Y, Yawata H, Kawanishi Y, Seed B, Taniguchi T, Hirano T, Kishimoto T. 1988. Cloning and expression of the human interleukin-6 (BSF-2/IFNβ 2) receptor. *Science 241*:825–828.

Yasueda H, Miyasaka Y, Shimamura T, Matsui H. 1992. Effect of semi-random mutagenesis at the C-terminal 4 amino acids of human interleukin-6 on its biological activity. *Biochem Biophys Res Commun 187*: 18–25.

Yasukawa K, Saito T, Fukunaga T, Sekimori Y, Koishihara Y, Fukui H, Ohsugi Y, Matsuda T, Yawata H, Hirano T, Taga T, Kishimoto T. 1990. Purification and characterization of soluble human IL-6 receptor expressed in CHO cells. *J Biochem 108*:673–676.

Zhang JG, Moritz RL, Reid GE, Ward LD, Simpson RJ. 1992. Purification and characterization of a recombinant murine interleukin-6: Isolation of N- and C-terminally truncated forms. *Eur J Biochem 207*:903–913.

Zhang JG, Reid GE, Moritz RL, Ward LD, Simpson RJ. 1993. Specific covalent modification of the tryptophan residues in murine interleukin-6. *Eur J Biochem 217*:53–59.

Note added in proof

Using human/mouse IL-6 chimeras, Ehlers et al. (1994, *J Immunol 153*:1744–1753) have recently shown that Gly 77–Glu 95 and Lys 41–Ala 56 of hIL-6 are involved in IL-6R binding and IL-6R-dependent complex formation with gp130, respectively.